15-Crown-5 Functionalized Au Nanoparticles Synthesized via Single Molecule Exchange on Silica Nanoparticles: Its Application to Probe 15-Crown-5/K^+/15-Crown-5 "Sandwiches" as Linking Mechanisms

Mei-Lin Ho, Jia-Ming Hsieh, Chih-Wei Lai, Hsin-Chieh Peng, Chia-Cheng Kang, I-Che Wu, Chin-Hung Lai, Yu-Chun Chen, and Pi-Tai Chou*

Department of Chemistry, National Taiwan University, Number 1, Section 4, Roosevelt Road, Da-an District, Taipei 106, Taiwan

Received: August 14, 2008; Revised Manuscript Received: November 26, 2008

Single 15-crown-5 functionalized Au nanoparticles (NPs) were synthesized with assistance of silica particles. The use of silica particles renders intrinsic advantages in that each step along the product formation can be monitored by, for example, a transmission electron microscope, and large surface-to-volume ratio of silica particles leads to a better yield of Au NP attachment than the glass substrate. The as prepared Au NPs, providing access to fundamental analysis, were readily applied in K^+ recognition and proved to be free from aggregation. Accordingly, a sandwich type of complexation is resolved and the corresponding thermodynamics can be extracted.

Introduction

The development of single molecule exchanged nanoparticles has received much attention in ion/molecular sensing. Among numerous methodologies, the exploitation of ionophores for the recognition site seems to be a promising area.[1] As for signal transducer, metal nanoparticles (NPs) emerge as an important role in colorimetry because of their high absorptivity and distinct color change that arises when switching between monodispersion and aggregation.[2−14] It is thus well-established that gold NPs can be functionalized with a monolayer of alkanethiols by virtue of the strong gold−sulfur bond,[15,16] in which thiolate ligands are strategically designed to provide recognition sites, namely, ionophores, for ion sensors. Among different ionophores, the crown ethers prefer complexation with different alkali metal ions and form stable chelation complexes.[17,18] For example, 18-crown-6 favors K^+ chelation and 15-crown-5 forms stable complex with Na^+. Furthermore, even though the cavity of a single 15-crown-5 (1.70−2.20 Å) is too small to accommodate K^+ (2.76 Å), the recognition of K^+ based on 15-crown-5 derivatives seems to be practical by introducing a 15-crown-5/K^+/15-crown-5 sandwich structure.[17−27]

Pompano et al.[28] reported crown ether ligands attached to monolayer-protected clusters (MPCs), which were assembled as films. The linking mechanism of the bridges, that is, crown ether/metal ion/crown ether "sandwiches", between nanoparticles was then examined. Kubo and co-workers[29] also reported discrete self-assembled systems using 15-crown-5-appended metalloporphyrins. The K^+ ion was sandwiched between two 15-crown-5 functional groups from two different porphyrin, and the outcome was a noncovalent tweezers-type bis(porphyrin). Janssen et al.[30] synthesized a chiral ditopic crown ether functionalized oligo(*p*-phenylenevinylene) (COPV). Via functionalizing the benzo-15-crown-5 moieties, COPV was capable of binding cations in chloroform. In the case of K^+ coordination, a strong 2:2 complex is formed, in which two COPVs are sandwiched between two potassium ions.

* Corresponding author. Fax: +886-2-23695208. Phone: +886-2-33663894. E-mail: chop@ntu.edu.tw.

As for a brief review of the nanoparticle being applied for K^+ recognition, Lin et al.[17,31] used 15-crown-5 capped Au NPs to detect K^+, in which a color change in solution from red to purple−blue was promptly observed upon adding K^+. The color switching was due to aggregation of gold NPs induced by 2:1 sandwich complex between 15-crown-5 moiety and K^+. Upon addition of, for example, 0.1 mM K^+, surface plasmon resonance (SPR) band absorbance at 528 nm decreases, accompanied by the appearance of a ∼710 nm band due to the coupled plasmon absorbance of NPs in close contact.[32] Previously, we reported the synthesis of two different sizes of CdSe/ZnS quantum dots (QDs) modified with 15-crown-5, and their capability of serving as a recognition unit for K^+ in aqueous solution.[33] The principle of K^+ identification lies in Förster type resonance energy transfer between two neighboring CdSe/ZnS QDs that are bridged by a sandwich complex of 15-crown-5 and K^+. The results offer a potential for differentiating ratiometric changes of dual emission (yellow and red) intensity as a function of K^+ concentrations.

For either Au NPs or CdSe/ZnS QDs systems, upon both 15-crown-5 capped Au NPs and CdSe/ZnS QDs were virtually networked via mutual sandwich complexation. The net result was severe aggregation due to multiple anchored ligands on each Au NPs (or CdSe/ZnS QDs). As a result, the cross conjugation of Au NPs takes place randomly upon association with K^+. Two possible binding schemes for sandwich complexation have been proposed,[24,25] namely, intraparticle and interparticle association. The former (intraparticle) case incorporated two 15-crown-5 molecules from neighboring arms of the same NPs (QDs) sandwiching a K^+ ion. In the latter (interparticle) case, two distinct 15-crown-5 molecules, originating from different NPs (QDs), formed an intermolecular type of association. The intraparticle association may give negligible color changes, as supported by several previous results. For example, in the study of 15-crown-5-QDs capped CdSe/ZnS recognizing K^+, when a low concentration of 15-crown-5-QDs capped CdSe/ZnS QDs was prepared and titrated by K^+, such that most of K^+ is assumed to be sandwiched with an intraparticle configuration, negligible spectral changes in both absorption and emission were observed.[33] As for another

10.1021/jp807256h CCC: $40.75
Published on Web 01/09/2009

example, in the study of chiral ditopic crown ether functionalized oligo(p-phenylenevinylene) (COPV) sensing Na^+, Janssen et al.[30] reported that Na^+ is bound, following a two-step negative cooperative process to form a 2:1 Na^+/COPV complex. This case is qualitatively similar to the intraparticle association. Their results show that binding of dual Na^+ intramolecularly has a marginal effect on the optical properties, a result that has been observed earlier for crown ether-appended dyes.[34] As for a complicated situation, due to multiligand association and aggregation effect, further fundamental studies on single molecular behavior during complexation are not feasible.

To gain insight into the association mechanism at the molecular level, functionalization of single 15-crown-5 anchored on individual metal/semiconductor NPs seems to be crucial.[35] Recently, through strategic chemical modification, anchoring a specific number of ligands on metal/semiconductor NPs became feasible.[36−38] Sung et al.[37] synthesized ∼2-nm sized Lys-monofunctionalized gold NPs by using PS Wang resin or HMPA-PEGA. Moreover, based on a solid phase approach, that is, a silane functionalized glass surface, Shumaker-Parry and co-workers[36] reported an elegant synthesis of Au NP dimers by adopting a coupling reaction of asymmetrically functionalized particles. Herein, we report the synthesis of single 15-crown-5 capped Au NPs by using silica particles as a solid-phase support. In comparison with the glass substrate, larger surface-to-volume ratio and the curved surface of silica particles might be advantageous during the reaction of single molecule exchange. Accordingly, the as prepared single 15-crown-5 functionalized gold NPs were successfully applied in the K^+ recognition, from which the associated thermodynamics can thus be deduced and discussed under a fundamental basis.

Experimental Section

The gold NPs with desired diameter were synthesized according to previous report.[39] The synthesis of silica particles was based on the previous report of Santra et al.[40] with slight modification. In brief, 2 g of triton X-100 (Aldrich), 8 mL of cyclohexane (Merck), and 1.6 mL of *n*-hexanol (Acros) were mixed with 0.34 mL of DI water for 3 h. Subsequently, 50 μL TEOS (Aldrich) was added to the solution and allowed to react for an additional 3 h. To initiate the TEOS hydrolysis, 100 μL of NH_4OH were added to the solution. After stirring for 24 h, the reaction was then terminated by the addition of ethanol. The silica particles were separated by centrifugation and redispersed in DI water. For coating the amino group on the surface of silica particles, 3-amino-propyltrimethoxysilane (10 μL) was added to a mixture of ethanol (30 mL), DI water (6 mL), NH_4OH (300 μL), and silica particles (20 mg). After 24 h, the sample was centrifuged several times to remove the unreacted chemicals. The precipitate of silica particles was then collected and redispersed in DI water. Subsequently, 6 mL of the gold NPs solution was injected into 30 mL of the as prepared silicon submicrometer-sized particle solution. The mixture was allowed to stir vigorously for 8 h. Owing to the amine groups, gold NPs were immobilized on the surface of silica particles. Gold NPs attached silica nanoclusters were then purified by using centrifugation to remove the free gold NPs remaining in water. After two purifications, silica-Au nanoclusters were immersed in 100 mM 2-mercaptoethanol solution for 6 h to replace all citric acid groups on the gold NPs surface, with an exception of stabilized sites between the amine groups (on silica surface) and the gold NPs.

After removal of bound-free thiol ligands by centrifugation at 1500 rpm, the thiol-capped gold-SiO_2 nanoclusters were then sonicated for the purpose of detaching gold NPs from SiO_2 surface. By a 1500 rpm centrifugation, the thiol-capped gold NPs solution was allowed to separate from the precipitation of SiO_2 particles. Next, by mixing thiol-capped gold NPs solution with 1 mM dithiol-modified 15-crown-5 ether solution for 30 min, the solution was collected to yield single dithiol-modified 15-crown-5 ether capped gold NPs. Since the outer surface of gold NPs has been occupied by a strong Au-thiol bond, the dithiol-modified 15-crown-5 ether could only attack the empty site formed by the detaching of SiO_2-NH_2. In each process, the shapes and size distributions of gold and silica particles were monitored with a JEOL JEM 1230 transmission electron microscope (TEM).

Results and Discussion

Scheme 1 depicts the synthetic routes of dithiol-modified single 15-crown-5 ether capped gold NPs. For clarity, the synthetic protocol is divided into four steps. For the first step (step 1), the anchoring of citric acid capped Au NPs ($\sim 4.0 \pm 1.0$ nm) on the alkylamino modified silica particles was achieved because of the stabilization energy between the Au NPs and the $-NH_2$ functional group on the surface of silica particles. Figure 1a shows a TEM image of Au NPs free, alkylamino surface-modified silica particles, the size of which was measured to be 90 ± 10 nm in diameter. Its amorphous property is supported by the X-ray diffraction pattern (see Figure S1 in Supporting Information). The TEM image shown in Figure 1b unveils the success of Au NPs anchored on the silica particles, in which the Au NPs are spread over the surface of silica particles. Optically, this is also supported by the bathochromic shift of surface plasmon resonance absorption band from 514 nm (black line, free Au NPs in water) to 517 nm for Au NPs on the surface of silica particles (red line, see Figure 2), providing that certain Au NPs on the silica surface may be close enough to induce certain SPR interactions. As the distance becomes smaller than the sum of the radii of two Au NPs, a simple quasistaic-limit approach based on the Mie's theory[41,42] predicts a red shift and a decrease in intensity of SPR transition (vide infra). According the Sardar et al.,[36] the plasmon absorption shift between citrate-stabilized 41 nm-diameter Au NPs on a silanized glass surface and thiol molecules on the outer surface of the closely packed nanoparticles was as small as 7 nm. Similar to that reported by Sarder et al., in our results, the absorption shift due to the SPR is not obvious. This can be rationalized based on recent results reported by Jain et al.[43] They pointed out that the decay length is roughly about 0.2 in units of the particle size for different nanoparticle size, shape, metal type, or medium dielectric constant. In our case, the distance (edge-to-edge) between Au and Au particles is longer than the decay length (0.8 nm, see Figure 1b), while the diameter of Au is 4 nm. As a result, the magnitude of the observed spectral shift is small due to a relatively weak near-field plasmon coupling.[44]

Step 2 involved the substitution of citric acids by 2-mercaptoethanol. The thiol-capped Au-NPs remaining on the silica particles were then monitored by TEM, as shown in Figure 1c. It is noteworthy that step 2 is to enhance the Au-ligand strength by invoking the relatively strong Au−S bonding. Attempts have also been made by directly using 2-mercaptoethanol modified Au NPs to attach on the silica particles. Unfortunately, as indicated by TEM image (see Figure S2, Supporting Information), we failed to obtain good-quality Au NP capped silica particles, plausibly due to the strong Au−S bonding strength that cannot be replaced via the $-NH_2$/Au interaction. As for

SCHEME 1: Synthesis Procedures of Single 15-Crown-5 Functionalized Au Nanoparticles and a Sandwich Au−K^+−Au Model for Potassium Ion Recognition

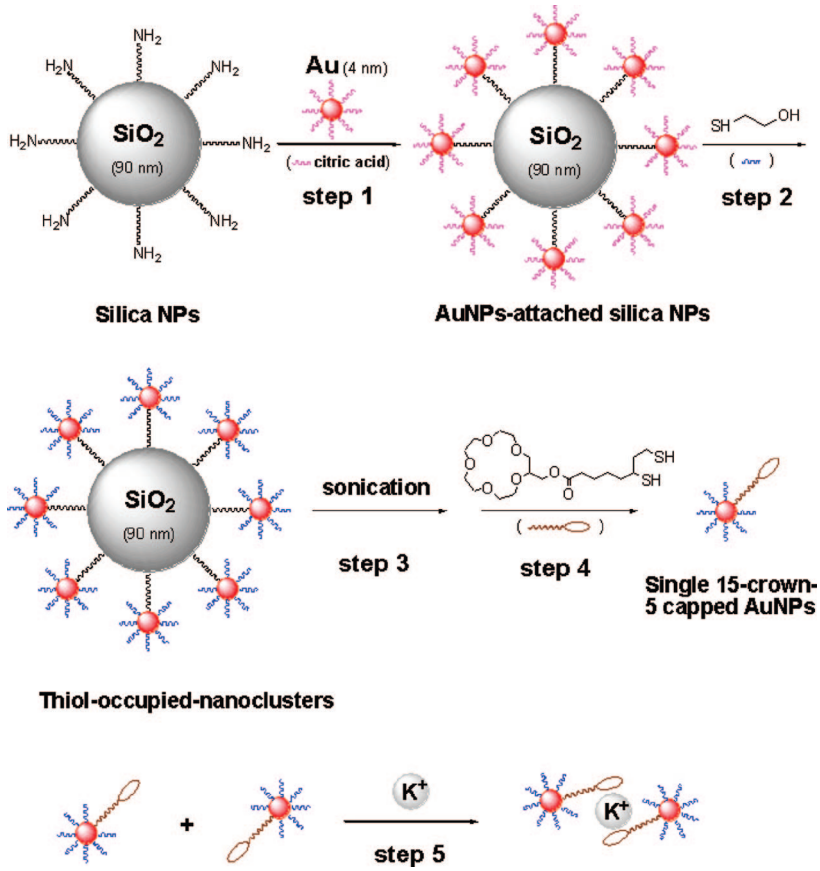

step 3, thiol-capped Au-NPs were detached from the silica particles via sonication, yielding the vacant site. This process was also supported by the TEM image provided in Figure 1d, in which the TEM image of precipitate was taken after the solution was centrifuged, showing only silica particle with negligible Au NPs on the surface. The suspension was then collected for the next step. As for step 4, we then introduced dithiol-modified 15-crown-5 ether to the solution containing thiolalcohol capped Au NPs. Upon stirring, the vacant site was then attached by Au-thiol-15-crown-5 ether bonding. According to previous results reported by Lin et al.[45a] and Wu et al.,[45b] employment of thiotic acid to modify Au NPs offers the advantages of stability that arises from the bidentate S−Au ligation with the negative charges. As shown in Figure 1e, the TEM image of the remaining solution reveals homogeneous dispersion of dithiol-modified 15-crown-5 ether capped Au NPs free from silica particles. Supplementary support is also given by the absorption measurement (Figure 2), in which the SPR peak was regained at ~525 nm (blue line), characteristic of Au NPs free from interparticle interactions. Nevertheless, in comparison to the citric acid capped Au NPs (black line), a slight red shift of ~10 nm was observed, which is likely due to a change of refractive index caused by thiol adsorption on the NPs surface.[36] Further information is also given by the histogram analysis (see Supporting Information, Figure S3), the result of which indicated that thiol-capped Au NPs size distribution was retained to be 4.0 ± 1.0 nm. Note that histograms regarding the particle size distribution are constructed based on four TEM photographs, and a total of 105 particles is used in this histogram. The unchanged particle-size distribution also eliminates the possibility that the red shift of SPR peak originates from the size enlargement of Au NPs.

In a brief summary, two advantages of the above-mentioned synthetic protocol can be pointed out. First, one can monitor the reaction in each step en route to the final product formation. Second, in comparison to silane functionalized glass surface, the use of silica submicrometer-sized particle (~90 nm) as a support may offer an advantage of large surface-to-volume ratio, which in theory leads to a higher product yield than the use of a glass substrate. Moreover, though pending proof, in comparison to the flat glass surface, the surface curvature provided by silica particles may allow a more specific single silica NP−NH_2−Au NP linkage and hence single dithiol modified 15-crown-5 ether capped Au NP production.

A control experiment in an aim to verify the single/multiple exchange of ligands on Au NPs was then performed. Because of the system complexity, our first attempts using ^{1}H NMR showed large spectral congestion, and hence data could not be used to extract valuable information. Alternatively, we then pursued IR spectroscopic study. In this approach, the single/multiple exchange of ligands on Au NPs experiment was performed by the protocol described above (steps 1 and 2). After sonication to release the Au NPs from SiO_2, we then exposed 2-mercaptoethanol capped Au NPs with vacancies to a solution of 2-mercaptoethanol and stirred for 12 h. The Au NPs, which are supposed to be fully capped by 2-mercaptoethanol, were then centrifuged for 10 min (at 10,000 rpm), followed by decantation of supernatants. As for further purification and IR measurement, 2-mercaptoethanol-stabilized Au NPs were purified by centrifugation, lyophilized, and deposited in a KBr pallet. This sample was then used as a control experiment, for which the transmission IR spectrum is shown in Figure 3 (see spectrum C).

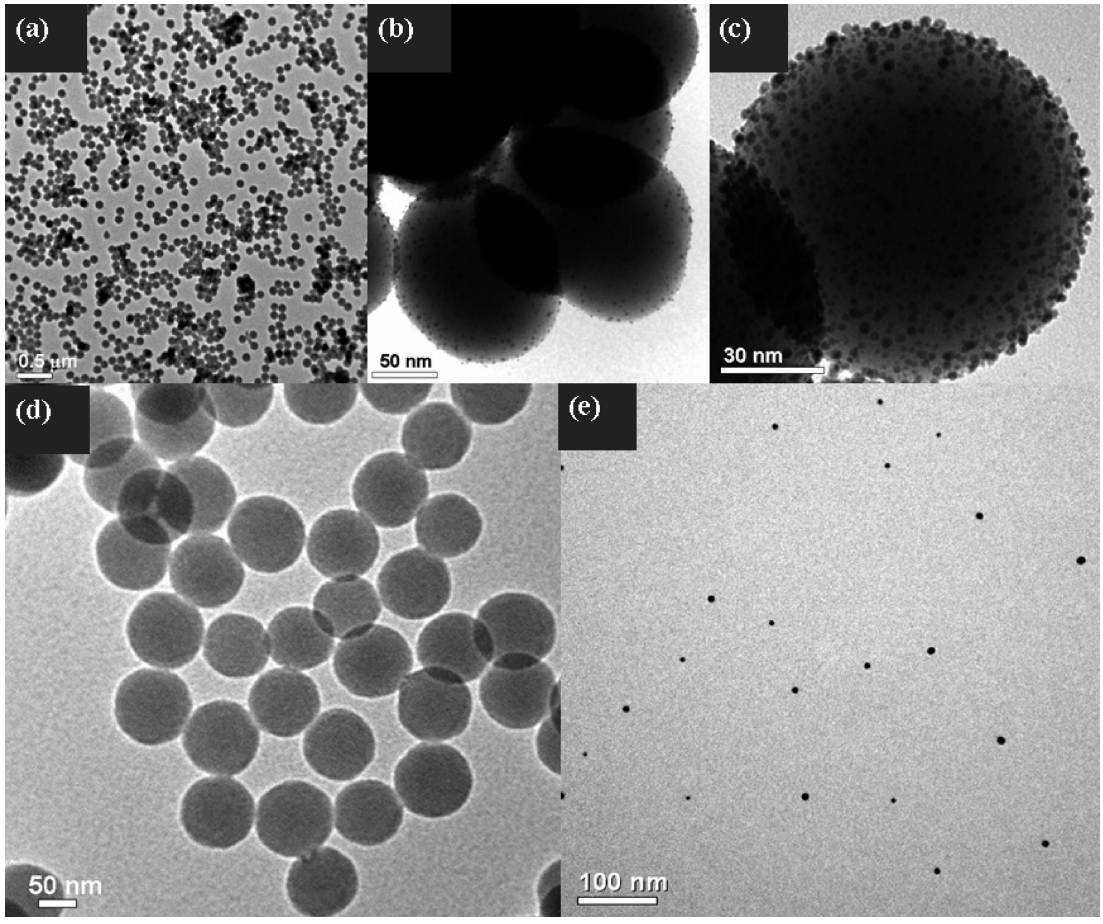

Figure 1. TEM of (a) non-Au capped Silica particles, (b) Au capped Silica paticles, (c) thiol-occupied-nanocluster, (d) the silica particles after detaching Au, and (e) single 15-crown-5 capped Au NPs.

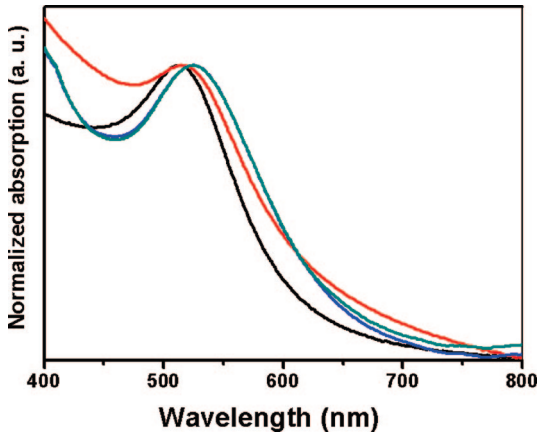

Figure 2. Normalized UV−visible absorption spectrum of Au NPs in each synthetic step: (black) pure Au NPs, (red) Au-NPs-attached silica particles, (blue) single 15-crown-5 capped Au NPs, and (green) single 15-crown-5 capped Au NPs after addition of 3×10^{-2} M K^+.

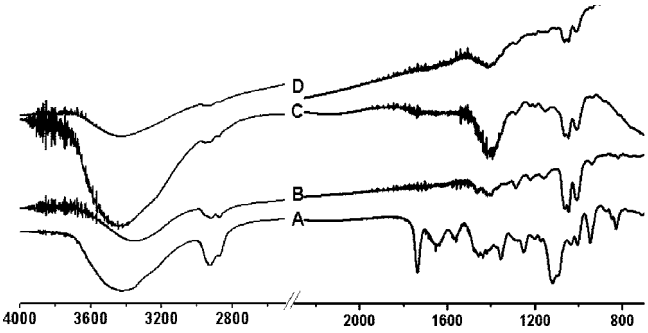

Figure 3. Transmission FTIR spectra of (A) dithiol-modified 15-crown-5 ether, (B) 2-mercaptoethanol, (C) 2-mercaptoethanol-stabilized Au NPs, and (D) dithiol-modified 15-crown-5 ether-stabilized Au NPs.

The as prepared 2-mercaptoethanol-stabilized Au NPs were then exposed to a solution of dithiol-modified 15-crown-5 ether (dithiol-modified 15-crown-5 ether-stabilized Au NPs), followed by a similar step described above for measuring the IR spectrum. The result is shown in Figure 3, spectral line D. For a fair comparison, IR spectra of standard dithiol-modified 15-crown-5 ether and 2-mercaptoethanol were also acquired and are depicted in lines A and B, respectively. Similar to Lin et al.[45] and our previous reports,[33,46] the IR absorption around 3420 cm^{-1} is a result of residual moisture within the dried NPs. The peaks at 2926 cm^{-1} and 2872 cm^{-1} are assigned to the vibrational modes of $\nu_{asy}(CH_2)$ and $\nu_{sym}(CH_2)$, respectively. Line A shows characteristic 1737 cm^{-1} absorption peak ascribed to C═O stretching motion of the ester functional group. This stretching mode clearly disappears at lines B, C, and D. More importantly, the spectral resemblance between line C and line D supports an attachment of single exchange of ligands on Au NPs.

In an aim to examine the uniqueness of single molecule exchange property, we then performed the K^+ recognition experiment to test 5-crown-5/K^+/15-crown-5 "sandwich" structure. The absorption titration spectra recorded for the single 15-crown-5 ether functionalized Au NPs as a function of $KClO_4$ concentrations (in pH = 7.2) are depicted in Figure 4. Upon increasing K^+ concentration, the decrease of 525 nm SPR band is due to the decrease of Au NPs monomer during titration, the

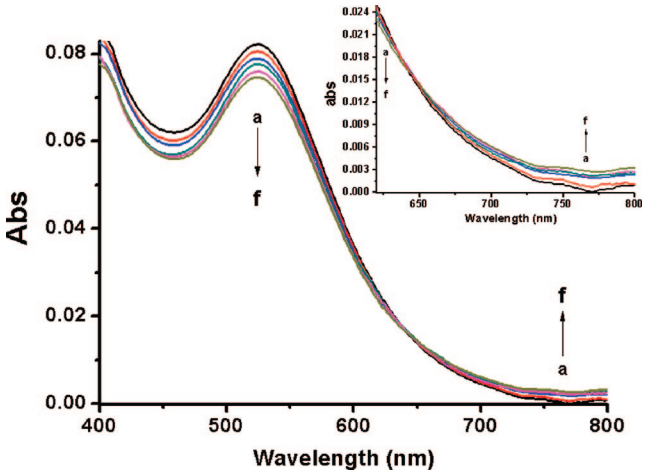

Figure 4. Absorption spectrum changes of Au monomer (1.8×10^{-9} M) upon addition of various concentrations of anhydrous $KClO_4$ in H_2O (pH ~ 7.2) (a) 0, (b) 1.50×10^{-4}, (c) 1.65×10^{-3}, (d) 5.05×10^{-3}, (e) 7.55×10^{-3}, and (f) 1.17×10^{-2} M. Note that the increase of volume for the titrant has been corrected. Inset: the enlargement of $\lambda > 630$ nm.

result of which is accompanied by an increase of absorbance at >610 nm associated with 15-crown-5/K^+/15-crown-5 sandwich formation. Previous studies have shown that plasmon resonance frequency depends on the nanoparticle composition, size, shape, local dielectric environment, and electromagnetic coupling to other proximate nanoparticles.[47−50] Some reports do indicate that as interparticle spacing decreases there is an expected shift in the λ_{max} of SPR,[44,51,52] For example, Reinhard et al.[51] reported detailed plasmon peak versus separation calibration curves for 42 and 87 nm diameter particle pairs. They also pointed out that the accuracy of absolute distance measurements is limited, in principle, by the possibility of multiple tether formation between nanoparticles. Any variation of the number of tethers between particles may broaden the distribution of the measured resonance wavelengths at a given spacer length.

In yet another approach, Jain et al.[52] have measured localized surface plasmon resonance (LSPR) in lithographically fabricated gold nanodisc (diameter 88 nm) pairs. Under parallel polarization, the plasmon resonance showed appreciable red shifts as the interparticle gap is reduced. In contrast, there is a very weak blue shift with decreasing gap for orthogonal polarization. They also performed the discrete approximation method toward a pair of diameter 10 nm Au nanospheres and found that the magnitude of the plasmon shift was much smaller than the 88 nm nanodisc pairs, possibly due to the smaller volume. Accordingly, they conclude that the fractional plasmon wavelength shifts along the interparticle axis decay exponentially with the interparticle gap, and the decay length is roughly about 0.2 in units of the particle size. Subsequently, Chen et al.[44] reported similar results as Jain et al.[52] and conclude that it would be very difficult to observe the near-field coupling effects for nanoparticle superlattices with diameter of ≤5 nm. Also, Reinhard et al.[51] pointed out that experimental polarization effects have low significance for nanoparticles of <40 nm in diameter.

On the above basis, the lack of obvious spectral shift in Figure 4 can be rationalized by a combination of two factors, namely, the polarization and size effect. As the size of the Au core is reduced to as small as ~4 nm, both size and polarization effects are negligible, resulting in a rather small shift in the SPR. Nevertheless, we also cannot eliminate another factor resulting from random motion of the K^+ sandwiched bridge in solution, the result of which, in part, may obscure the spectral shift.

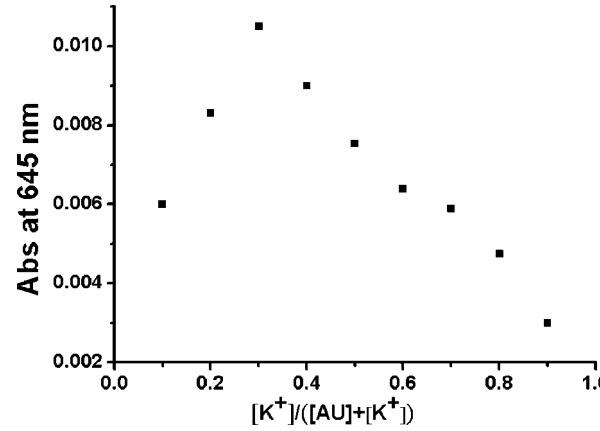

Figure 5. Job's plot of a 2:1 complex of Au and K^+. [Au] + [K^+] = 1.78 nM. The absorbance is monitored at 645 nm.

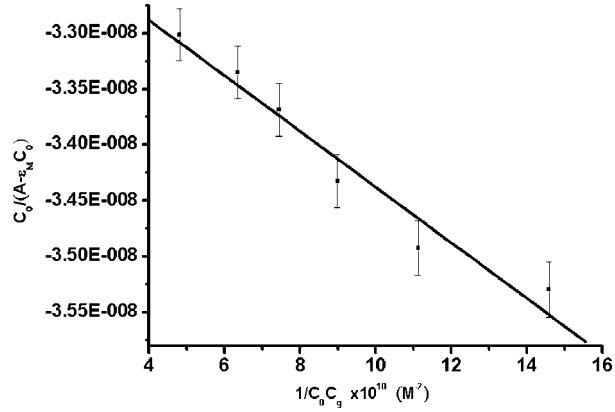

Figure 6. Plot of $C_0/(A_{522} - \epsilon_M C_0)$ against $1/C_0C_g$ at 522 nm. See text for the definition of parameters.

The concentration of Au NPs was then calculated by adopting the Beer−Lambert law, and the extinction coefficient (ε_M) of the as prepared ~4 nm Au monomer was estimated to be 7×10^7 M^{-1} cm^{-1} at the 516 nm of SPR band.[6,53] It is noteworthy that the molar extinction coefficient of Au SPR band, in theory, is proportional to their diameter.[6,53] In addition, Figure 5 shows a plot of absorbance at 645 nm against the mole fractions of K^+ under a constant concentration of [Au NPs] + [K^+]. As shown in Figure 5, a Job's plot analysis[54] was then performed with an aim to verify the reaction stoichiometry. It is obvious that the concentration of Au−K^+ complex reached a maximum value when the molar fraction [K^+]/([Au NP] + [K^+]) was about 0.3, indicating a 1(K^+):2(Au NP) stoichiometry for the complexation. Since 15-crown-5 cavity is too small to accommodate K^+, a sandwich type of Au NP/K^+/Au NP configuration seems to be the most acceptable model.

Bearing the 1(K^+):2(Au NP) association stoichiometry in mind, the relationship among absorbance of the mixture (A), the initially prepared Au NPs concentration (C_0), and the concentration of K^+ (C_g) can be expressed by

$$\frac{C_0}{A - \varepsilon_M C_0} = \left[\frac{1}{K_a(\varepsilon_D - 2\varepsilon_M)}\right]\frac{1}{C_0 C_g} + \frac{4}{\varepsilon_D - 2\varepsilon_M} \qquad (1)$$

where ϵ_M and ϵ_D are molar extinction coefficients of the monomeric Au NP and Au NP/K^+/Au NP complex, respectively, at a specific wavelength. Detailed derivation of eq 1 is elaborated in Supporting Information. The plot of $C_0/(A_{522}\epsilon_M C_0)$ as a function $1/C_0C_g$ (Figure 6) reveals a straight line, further supporting the 1(K^+):2(Au NP) reaction stoichiometry. The

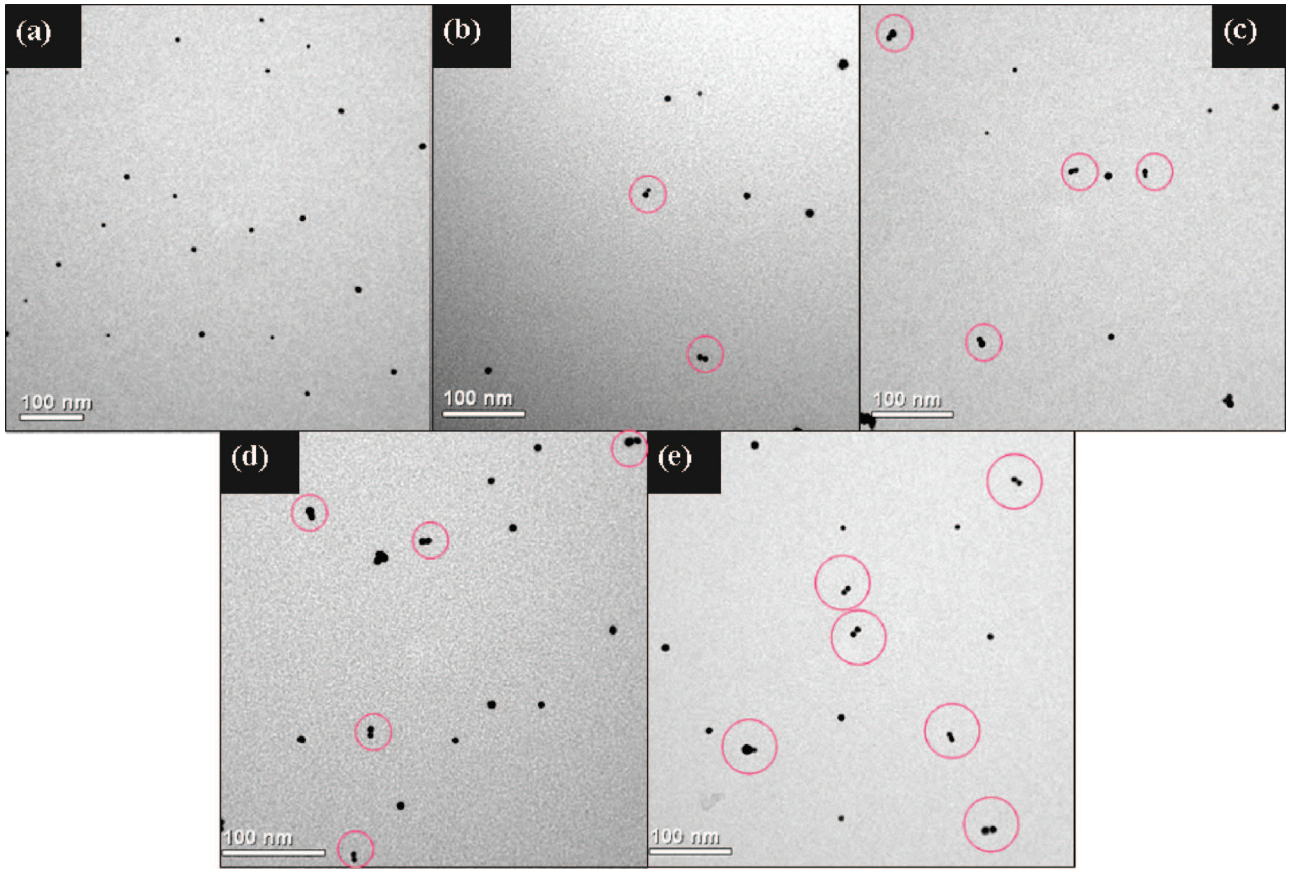

Figure 7. TEM of single 15-crown-5 capped Au NPs are titrated with increasing concentration of K^+. (a) 0, (b) 5.00×10^{-5}, (c) 1.50×10^{-4}, (d) 2.00×10^{-3}, and (e) 8.00×10^{-3} M K^+.

association constant K_a can thus be calculated to be 32 ± 10 M^{-2}, extracted from intercept/[4 × slope]. This value, within experimental error, seems to be larger than the K_a value of 5.5−5.7 M^{-2} reported from the K^+ recognition based on the ligand of 15-crown-5 unit.[31,55,56] The discrepancy in binding affinity between single molecule functionalized Au-NPs and single molecular systems may manifest the entropy factor governing the recognition reaction. Beer et al.[57] have successfully demonstrated that the binding affinities toward anion sensing is significantly enhanced when the receptor, zinc metalloporphyrins, was placed onto gold nanoparticle surfaces relative to the free metallophorphyrins;[57] for example, comparing that of the zinc metalloporphyrin, the binding affinities of chloride is more than two orders of magnitude larger when using the surface-confined porphyrin-functionalized NPs. Such an increase in association upon confining the receptor to a surface has been rationalized by factors controlling enthalpy and entropy during the host/guest recognition reaction.[58] Via preorganization of receptors on surfaces, thereby reducing their conformational flexibility, that is, a contribution that increases the energetic cost of association, the entropic contributions would be expected to be more favorable. This mechanism, in part, has been adopted for multi-15-crown-5 functionalized Au NPs in K^+ recognition to explain its ultrasensitive color changes, although it is not feasible to resolve the association thermodynamics due to the complicated association and aggregation, followed by precipitation.[17,31] In comparison to free 15-crown-5 receptor,[31,55] the sixfold increase in the association constant for single 15-crown-5 functionalized Au NPs may not be dramatic. The result implicitly implies more conformational flexibility in single 15-crown-5 functionalized Au NPs versus that of multi-15-crown-5 functionalized Au NPs.

The K^+ recognition utilizing single 15-crown-5 functionalized Au NPs offers a unique advantage toward manipulating the complexation "visualized" via TEM, the results of which should provide a supplementary support for sandwich type of recognition mechanism. Figure 7a−e unveils TEM images of single 15-crown-5 functionalized Au NPs as a function of the added K^+ concentrations. Although TEM images only represents a small part of the deposited solution and the dispersion of Au NPs on the copper mash may not be homogeneous, in a qualitative manner, the percentage of Au NP dimer increased upon adding [K^+] from 0 (Figure 7a) to 8.00×10^{-3} M (Figure 7e). Moreover, in sharp contrast to Figure 7a, which reveals a homogeneous dispersion of monomeric Au NP, a great portion of dimeric Au NPs could be found in TEM image shown in Figure 7e upon titration with 8.00×10^{-3} M K^+. As for a simplified approach, the yield of dimeric formation observed in TEM images is defined as the ratio of dimers versus the total number of structures where single particles, dimers, trimers, and other clusters were counted as unique structures. In addition, the yield of each batch of dimers was averaged by counting at least 100 particles from 20 to 25 TEM images of the same sample. Accordingly, the yield of Au NP/K^+/Au NP sandwich (4−4 nm) was estimated to be ∼70% upon adding [K^+] to 8.00×10^{-3} M. Distance measurement between Au−K^+−Au sandwich is from TEM analysis (Figure 7 and Figure S4, Supporting Information). We then measured the spacing between two Au particles (among ∼50 pairs) to be within a range of 1.2∼2.0 nm. This fluctuation is expectable, considering the statistically twist of the structure caused by the formation of four Au−S bonds. In yet another approach, we assumed that the complex of K^+ with two molecules of dithol-modified 15-crown-5 ether immersed in a spherical cavity and then performed

semiempirical AM1 optimization.[59] Accordingly, the diameter of the cavity was calculated to be 1.5 nm, which is in agreement with that (1.2−2.0 nm) of TEM analyses. Accordingly, Au NP/K^+/Au NP framework bridged by dual 15-crown-5 in a sandwich-like structure is justified via visualization.

Conclusion

In summary, we report the synthetic protocol of 15-crown-5 functionalized Au nanoparticles via a single molecule exchange method and its application in 15-crown-5/K^+/15-crown-5 recognition to visualize the sandwich as the linking mechanism. This method incorporating silica particle as a support offers the advantages of TEM visualization and UV−vis changes en route to product formation, such that each step can be optimized. Large surface-to-volume ratio, in theory, also improves production yield. On this basis, we then demonstrated a prototypical application of single 15-crown-5 capped Au NPs for potassium ion recognition in aqueous solution. Supported by a Job's plot and TEM image, Au NP/K^+/Au NP sandwich-like configuration is then established.

One may cast doubt on practical applications regarding the single ligand (15-crown-5) functionalized Au NPs. Multiple 15-crown-5 capped Au NP might render its advantage in view of color visualization and hence the sensitivity amid K^+ recognition. This is expected because of the fact that, induced by the 2:1 sandwich complexation, severe interparticle aggregation among multiple 15-crown-5 capped Au NPs should take place, enhancing the Au NPs in close contact. As a result, the decrease of SPR absorbance and the accompanied increase of absorbance at, for example, >600 nm due to the cross SPR interaction should be more pronounced. However, single 15-crown-5 capped Au NP offers its advantage toward the fundamental approach such as the associated thermodynamics and TEM visualization of the dimeric form demonstrated in this study. Future extension of single ligand functionalized NPs are versatile, for example, the dynamics of energy transfer between Au and Au NPs (surface energy transfer), Au NPs and semiconductor NPs, semiconductor NPs and semiconductor NPs (Förster type of resonance energy transfer) as well as the fundamental of electron/energy transfer between NPs. In yet another research area, through chemical modification, that is, a bottom-up approach, rational design to assemble the architecture of nanomaterials may become feasible, and their associated motion may be visualized via the access of suitable nanotechnologies. We may thus foresee the perspective of synthesizing nanoframework (product) based on each nanounit (reagents) with a rational way akin to the organic/inorganic synthesis at the molecular level.

Acknowledgment. Generous support from the National Science Council of Taiwan is acknowledged.

Supporting Information Available: XRD and TEM images, histogram analysis, and the derivation of the association constant of Au−K^+−Au dimer. This material is available free of charge via the Internet at http://pubs.acs.org.

References and Notes

(1) Steed, J. W.; Atwood, J. L. *Supramolecular Chemistry*; John Wiley & Sons: New York, 2000.
(2) Brust, M.; Bethell, D.; Schiffren, D. J.; Kiely, C. J. *Adv. Mater.* **1995**, *7*, 795.
(3) Grabar, K. C.; Freeman, R. G.; Hommer, M. B.; Natan, M. *J. Anal. Chem.* **1995**, *67*, 735.
(4) Mirkin, C. A.; Letsinger, R. L.; Mucic, R. C.; Storhoff, J. J. *Nature* **1996**, *382*, 607.
(5) Elghanian, R.; Storhoff, J. J.; Mucic, R. C.; Letsinger, R. L.; Mirkin, C. A. *Science* **1997**, *277*, 1078.
(6) Link, S.; El-Sayed, M. A. *J. Phys. Chem. B* **1999**, *103*, 8410.
(7) Demers, L. M.; Mirkin, C. A.; Mucic, R. C.; Reynolds III, R. A.; Letsinger, R. L.; Elghanian, R.; Viswanadham, G. *Anal. Chem.* **2000**, *72*, 5535.
(8) Kim, Y.; Johnson, R. C.; Hupp, J. T. *Nano Lett.* **2001**, *1*, 165.
(9) Niemeyer, C. M. *Angew. Chem.* **2001**, *113*, 4254. Angew. Chem., Int. Ed. 2001, *40*, 4128.
(10) Shenhar, R.; Rotello, V. M. *Acc. Chem. Res.* **2003**, *36*, 549.
(11) Daniel, M.-C.; Astruc, D. *Chem. Rev.* **2004**, *104*, 293.
(12) Rosi, N. L.; Mirkin, C. A. *Chem. Rev.* **2005**, *105*, 1547.
(13) Lee, J.-S.; Han, M. S.; Mirkin, C. A. *Angew. Chem., Int. Ed.* **2007**, *46*, 4093.
(14) Lee, J.-S.; Lytton-Jean, A. K. R.; Hurst, S. J.; Mirkin, C. A. *Nano Lett.* **2007**, *7*, 2112.
(15) Thomas, K. G.; Kamat, P. V. *Acc. Chem. Res.* **2003**, *36*, 888.
(16) Ohnuma, A.; Abe, R.; Shibayama, T.; Ohtani, B. *Chem. Commun.* **2007**, 3491.
(17) Lin, S.-Y.; Liu, S.-W.; Lin, C.-M.; Chen, C.-h. *Anal. Chem.* **2002**, *74*, 330.
(18) Gokel, G. W.; Leevy, W. M.; Weber, M. E. *Chem. Rev.* **2004**, *104*, 2723.
(19) Masilamani, D.; Lucas, M. E. *Fluorescent Chemosensors for Ion and Molecule Recognition*; Czarnik, A. W., Ed.; American Chemical Society: Washington, DC, 1992.
(20) Inoue, Y.; Gokel, G. W. *Cation Binding by Macrocycles: Complexation of Cationic Species by Crown Ethers*: Marcel Dekker: New York, 1990.
(21) Bradshaw, J. S.; Krakowiak, K. E.; Izatt, R. M. *Aza-Crown Macrocycles*; *John Wiley and Sons*: New York, 1993.
(22) Toupance, T.; Benoit, H.; Sarazin, D.; Simon, J. *J. Am. Chem. Soc.* **1997**, *119*, 9191.
(23) Boldea, A.; Levesque, I.; Leclerc, M. *J. Mater. Chem.* **1999**, *9*, 2133.
(24) Flink, S.; Boukamp, B. A.; van den Berg, A.; van Veggel, F. C. J. M.; Reinhoudt, D. N. *J. Am. Chem. Soc.* **1998**, *120*, 4652.
(25) Flink, S.; van Veggel, F. C. J. M.; Reinhoudt, D. N. *J. Phys. Chem. B* **1999**, *103*, 6515.
(26) Kimura, K.; Harino, H.; Hayata, E.; Shono, T. *Anal. Chem.* **1986**, *58*, 2233.
(27) Lin, S.-Y.; Wu, S.-H.; Chen, C.-h. *Angew. Chem., Int. Ed.* **2006**, *45*, 4948.
(28) Pompano, R. R.; Wortley, P. G.; Moatz, L. M.; Tognarelli, D. J.; Kittredge, K. W.; Leopold, M. C. *Thin Solid Films* **2006**, *510*, 311.
(29) Ishii, Y.; Soeda, Y.; Kubo, Y. *Chem. Commun.* **2007**, 2953.
(30) Janssen, P. G. A.; Jonkheijm, P.; Thordarson, P.; Gielen, J. C.; Christianen, P. C. M.; van Dongen, J. L. J.; Meijer, E. W.; Schenning, A. P. H. J. *J. Mater. Chem.* **2007**, *17*, 2654.
(31) Lin, S.-Y.; Chen, C.-h.; Lin, M.-C.; Hsu, H.-F. *Anal. Chem.* **2005**, *77*, 4821.
(32) Storhoff, J. J.; Lazarides, A. A.; Mucic, R. C.; Mirkin, C. A.; Letsinger, R. L.; Schatz, G. C. *J. Am. Chem. Soc.* **2000**, *122*, 4640.
(33) Chen, C.-Y.; Cheng, C.-T.; Lai, C.-W.; Wu, P.-W.; Wu, K.-C.; Chou, P.-T.; Chou, Y.-H.; Chiu, H.-T. *Chem. Commun.* **2006**, 263.
(34) Shinmori, H.; Yasuda, Y.; Osaka, A. *Eur. J. Org. Chem.* **2002**, 1197.
(35) Claridge, S. A.; Mastroianni, A. J.; Au, Y. B.; Liang, H. W.; Micheel, C. M.; Fréchet, J. M. J.; Alivisatos, A. P. *J. Am. Chem. Soc.* **2008**, *130* (29), 9598.
(36) Sardar, R.; Heap, T. B.; Shumaker-Parry, J. S. *J. Am. Chem. Soc.* **2007**, *129*, 5356.
(37) Sung, K. M.; Mosley, D. W.; Peelle, B. R.; Zhang, S.; Jacobson, J. M. *J. Am. Chem. Soc.* **2004**, *126*, 5064.
(38) Krüger, C.; Agarwal, S.; Greiner, A. *J. Am. Chem. Soc.* **2008**, *130*, 2710.
(39) Jana, N. R.; Gearheart, L.; Murphy, C. J. *J. Phys. Chem. B* **2001**, *105*, 4065.
(40) Santra, S.; Bagwe, R. P.; Dutta, D.; Stanley, J. T.; Walter, G. A.; Tan, W.; Moudgil, B. M.; Mericle, R. A. *Adv. Mater.* **2005**, *17*, 2165.
(41) Gluodenis, M.; Foss, C. A., Jr *J. Phys. Chem. B* **2002**, *106*, 9484.
(42) Mie, G. *Ann. Phys.* **1908**, *25*, 377.
(43) Jain, P. K.; Huang, W.; El-Sayed, M. A. *Nano Lett.* **2007**, *7*, 2080.
(44) Chen, C.-F.; Tzeng, S.-D.; Chen, H.-Y.; Lin, K.-J.; Gwo, S. *J. Am. Chem. Soc.* **2008**, *130*, 824.
(45) (a) Lin, S.-Y.; Tsai, Y.-T.; Chen, C.-C.; Lin, C.-M.; Chen, C.-h. *J. Phys. Chem. B* **2004**, *108*, 2134. (b) Wu, S.-H.; Wu, Y.-S.; Chen, C.-h. *Anal. Chem.* **2008**, *80*, 6560.
(46) Hsieh, J.-M.; Ho, M.-L.; Wu, P.-W.; Chou, P.-T.; Tsai, T.-T.; Chi, Y. *Chem. Commun.* **2006**, 615.
(47) (a) Kreibig, U.; Vollmer, M. *Optical Properties of Metal Clusters*; Springer-Verlag: Berlin, 1995. (b) Kelly, K. L.; Coronado, E.; Zhao, L. L.; Schatz, G. C. *J. Phys. Chem. B* **2003**, *107*, 668.

(48) Link, S.; El-Sayed, M. A. *J. Phys. Chem. B* **1999**, *103*, 4212.
(49) (a) Underwood, S.; Mulvaney, P. *Langmuir* **1994**, *10*, 3427. (b) Alvarez, M. M.; Khoury, J. T.; Schaaff, T. G.; Shafigullin, M. N.; Vezmar, I.; Whetten, R. L. S. *J. Phys. Chem. B* **1997**, *101*, 3706. (c) Templeton, A. C.; Pietron, J. J.; Murray, R. W.; Mulvaney, P. *J. Phys. Chem. B* **2000**, *104*, 564.
(50) (a) Taleb, A.; Petit, C.; Pileni, M. P. *J. Phys. Chem. B* **1998**, *102*, 2214. (b) Ung, T.; Liz-Marza′n, L. M.; Mulvaney, P. *J. Phys. Chem. B* **2001**, *105*, 3441. (c) Malynych, S.; Chumanov, G. *J. Am. Chem. Soc.* **2003**, *125*, 2896.
(51) Reinhard, B. M.; Siu, M.; Agarwal, H.; Alivisatos, A. P.; Liphardt, J. *Nano Lett.* **2005**, *5*, 2246.
(52) Jain, P. K.; Huang, W.; El-Sayed, M. A. *Nano Lett.* **2007**, *7*, 2080.
(53) Mulvaney, P. *Langmuir* **1996**, *12*, 788.
(54) Papavassiliou, G. C. *Prog. Solid State Chem.* **1980**, *12*, 185.
(55) Izatt, R. M.; Pawlak, K.; Bradshaw, J. S. *Chem. Rev.* **1991**, *91*, 1721.
(56) Mulvaney, P. *Langmuir* **1996**, *12*, 788.
(57) Beer, P. D.; Cormode, D. P.; Davis, J. J. *Chem. Commun.* **2004**, 414.
(58) Labande, A.; Ruiz, J.; Astruc, D. *J. Am. Chem. Soc.* **2002**, *124*, 1782. (a) Daniel, M.-C.; Ruiz, J.; Nlate, S.; Blais, J.-C.; Astruc, D. *J. Am. Chem. Soc.* **2003**, *125*, 2617.
(59) Dewar, M.; Thiel, W. *J. Am. Chem. Soc.* **1977**, *99*, 4499.

JP807256H